



Research article

Analysis of *SIGLEC12* expression, immunomodulation and prognostic value in renal cancer using multiomic databases

Amobichukwu K. Ogbodo^{a,f}, Denis Mustafov^{a,b}, Mohit Arora^c,
George I. Lambrou^{d,e}, Maria Braoudaki^a, Shoib S. Siddiqui^{a,*}

^a School of Life and Medical Sciences, University of Hertfordshire, College Lane Campus, Hatfield AL10 9AB, United Kingdom

^b College of Health, Medicine, and Life Science, Brunel University London UB8 3PH, United Kingdom

^c Department of Biochemistry, All India Institute of Medical Sciences, New Delhi 110029, India

^d Choremeio Research Laboratory, First Department of Paediatrics, School of Medicine, National and Kapodistrian University of Athens, Athens, Greece, Thivon & Levadeias 8, 11527, Goudi, Athens, Greece

^e University Research Institute of Maternal and Child Health & Precision Medicine, National and Kapodistrian University of Athens, Thivon & Levadeias 8, 11527 Athens, Greece

^f #Current Address: Nuffield Department of Population Health, University of Oxford, Richard Doll Building, Old Road Campus, Oxford OX3 7LF, United Kingdom

ARTICLE INFO

Keywords:

SIGLEC12

Immunotherapy

Carcinomas

Kidney

KM plotter

UALCAN

ABSTRACT

Siglecs belong to a family of immune regulatory receptors predominantly found on hematopoietic cells. They interact with Sia, resulting in the activation or inhibition of the immune response. Previous reports have suggested that the *SIGLEC12* gene, which encodes the Siglec-XII protein, is expressed in the epithelial tissues and upregulated in carcinomas. However, studies deciphering the role of Siglec-XII in renal cancer (RC) are still unavailable, and here we provide insights on this question. We conducted expression analysis using the Human Protein Atlas and UALCAN databases. The impact of *SIGLEC12* on RC prognosis was determined using the KM plotter, and an assessment of immune infiltration with *SIGLEC12* was performed using the TIMER database. GSEA was conducted to identify the pathways affected by *SIGLEC12*. Finally, using GeneMania, we identified Siglec-XII interacting proteins. Our findings indicated that macrophages express *SIGLEC12* in the kidney. Furthermore, we hypothesize that Siglec-XII expression might be involved in the increase of primary RC, but this effect may not be dependent on the age of the patient. In the tumour microenvironment, oncogenic pathways appeared to be upregulated by *SIGLEC12*. Similarly, our analysis suggested that *SIGLEC12*-related kidney renal papillary cell carcinomas may be more suitable for targeted immunotherapy, such as CTLA-4 and PD-1/PD-L1 inhibitors. These preliminary results suggested that high expression of *SIGLEC12* is associated with poor prognosis for RC. Future studies to assess its clinical utility are necessitated.

1. Introduction

Renal cancer (RC) is a common urological malignancy that poses a significant public health challenge due to its insidious nature and late diagnosis, making it one of the most challenging cancers to treat [1,2]. According to GLOBOCAN 2020 (Global Cancer

* Corresponding author.

E-mail address: s.siddiqui3@herts.ac.uk (S.S. Siddiqui).

<https://doi.org/10.1016/j.heliyon.2024.e24286>

Received 4 June 2023; Received in revised form 30 November 2023; Accepted 5 January 2024

Available online 11 January 2024

2405-8440/© 2024 The Author(s).

Published by Elsevier Ltd.

This is an open access article under the CC BY license

(<http://creativecommons.org/licenses/by/4.0/>).

List of abbreviations

Abbreviation Explanation

APCs	Antigen Presenting Cell
AKT	Protein Kinase B
ATCase	Aspartate transcarbamylase
BLCA	Bladder urothelial carcinoma
C	Breast invasive carcinoma tumour
ccRCC	Complement Clear Cell Renal Cell Carcinoma
CD33rSiglecs	CD33-Related Siglecs
CESC	Cervical squamous cell carcinoma
CHOL	Cholangiocarcinoma
CI	Confidence Interval
CNA	Copy Number Alteration
CNV	Copy Number Variation
COAD	Colon adenocarcinoma
CPS-II	Carbamoyl phosphate synthetase-II
CTLA-4	Cytotoxic T-lymphocyte-Associated Protein 4
EIF	Eukaryotic initiation factor
ESCA	Esophageal carcinoma
GBM	Glioblastoma multiforme
GLOBOCAN	Global Cancer Incidence, Mortality and Prevalence
GO	Gene Ontology
HNSC	Head and neck squamous cell carcinoma
HR	Hazard Ratio
IFN-γ	Interferon Gamma
IL-2	Interleukin 2
ITIMs	Immunoreceptor Tyrosine-based Inhibitory Motifs
KEGG	Kyoto Encyclopaedia of Genes and Genomes
KICH	Kidney chromophobe
KIRC	Kidney Renal Clear Cell Carcinoma
KIRP	Kidney Renal Papillary Cell Carcinoma
KM plotter	Kaplan–Meier Plotter
LIHC	Liver hepatocellular carcinoma
LUAD	Lung adenocarcinoma
LUSC	Lung squamous cell adenocarcinoma
MDSC	Myeloid-derived suppressor cells
NF-κB	Nuclear Factor Kappa B
ncRNAs	non-coding RNAs
nTPM	Consensus Normalized Transcript Expression
MTORC1	Mammalian Target of Rapamycin Complex 1
OS	Overall Survival
PAAD	Pancreatic adenocarcinoma
PCPG	Pheochromocytoma and paraganglioma
P13K	Prostrate adenocarcinoma Phosphoinositide 3-Kinases
PD-1/PD-L1	Programmed Death-1/Programmed Death-Ligand 1
PLAA	Phospholipase A2-Activating Protein
READ	Rectal adenocarcinoma
RC	Renal Cancer
RFS	Relapse Free Survival
SARC	Sarcoma
Sias	Sialic Acids
SKCM	Skin cutaneous melanoma
STAD	Stomach adenocarcinoma
STAT3	Signal Transducer and Activator of Transcription 3
THCA	Thyroid carcinoma
TME	Tumour Microenvironment
TNF	Tumour Necrosis Factor
THYM	Thyoma
UCEC	Uterine corpus endometrial carcinoma
WT	Wilms Tumour

Incidence, Mortality and Prevalence) data, more than 400,000 RC cases were diagnosed in 2020, resulting in approximately 180,000 deaths [3]. The geographical incidence varies significantly, with a high prevalence in North America, followed by Europe and Australia [4]. In contrast, the incidence in South America, Africa and Asia is considerably low [5]. RC is more prevalent in men than in women, ranking as the seventh and ninth most common cancer in these genders, respectively [6]. It is worth noting that undefined environmental factors, genetic predisposition syndromes such as genitourinary malformation or overgrowth, and molecular drivers involving more than 40 genes underpin the development of RC [7,8]. Importantly, RC is not a single disease but a collection of different heterogeneous cancer types that occur in one organ, each characterized by various genetic and phenotypic mutations [6].

Siglecs are cell-surface receptors expressed as immune checkpoints, typically on the surface of innate immune cells [9,10]. It has been reported that non-immune cells, such as ovarian fibroblast, intestinal M-cells, pancreatic α - and β -cells, can also express these proteins [11]. They bind with their ligands sialic acids (Sias), a family of glycans ubiquitously present at the terminal ends of the glycans chains on the cell surface and extracellular glycoconjugates [9]. Siglecs, which evolved from the duplication of the CD33 gene, are known as CD33-related Siglecs (CD33rSiglecs) or rapidly evolving Siglecs, while others are evolutionarily conserved [12]. In the cytosolic tail, the majority of CD33rSiglecs have immunoinhibitory functions mediated by immunoreceptor tyrosine-based inhibitory motifs (ITIMs) and ITIM-like motifs [13,14]. Through binding with preferred sialoglycans, they initiate intracellular signalling to recruit protein tyrosine phosphatases Src-homology 2 domain (SH2)-containing phosphatase 1 (SHP-1) and SHP-2, thereby participating in the numerous signalling cascades that influence cellular immune inhibition [9]. Report indicate that human Siglec-XII a family of CD33rSiglecs, is expressed in approximately ~30–40 % of the sub-Saharan African population, while a high incidence of about ~75–90 % expression is observed in the Native American populace [15].

However, Siglec-XII has been linked as a non-functional protein with atypism in different ways [15]. Firstly, it is unable to recognize Sias due to a human-universal mutation of critical arginine residues present in both domains of the V-set. As a result, Roman numeral XII is used for the protein, instead of Arabic numerals for Sia binding Siglecs [15]. Secondly, there is a polymorphic frameshift

mutation truncating Siglec-XII harboured by the *SIGLEC12* gene [16], resulting in the expression loss of the protein's full length in most humans [17]. Thirdly, the presence of two-amino-terminal V-set domains in the protein, whereas other Siglecs have only one [18]. Studies have also highlighted the possible functionality of this protein. Yu et al., (2001) suggested that human Siglec-XII has ITIM and ITIM-like domains in the cytosolic tail, which can be phosphorylated to recruit SHP-1 and SHP-2 phosphatases, even though it does not recognize Sias [18]. Genome-wide studies showed that polymorphism in the human population introduced nonsense-mediated decay into human genes, including *SIGLEC12* [19]. This may have resulted in *SIGLEC12* appearing to undergo selection favouring a null and/or truncated form [20]. Furthermore, studies on the frameshift polymorphism of *SIGLEC12* in the human population suggested rs16982743 as an inactivating mutation [19] and rs66949844 as a frameshift mutation [15]. Similarly, evidence of rare excess alleles in the genomic region indicates a low-level population differentiation, suggestive of balancing selection [21,22]. Other studies have shown that *SIGLEC12* appears to be an outlier among 167 genes studied for polymorphic nonsense single-nucleotide polymorphisms [19]. The statistical parameter called F_{ST} , which measures population differentiation, suggested mildly deleterious polymorphisms of most nonsense single nucleotide with a low F_{ST} value [17]. Contrastingly, *SIGLEC12* had a high F_{ST} and relatively high heterozygosity, which also are indicative of a selective sweep or balancing selection [17].

It has been demonstrated that the non-Sia-binding Siglec-XII can be expressed in transfected *SIGLEC12* mutated prostate cancer cell lines, leading to the dysregulation of oncogenic pathways and immune checkpoints [15]. However, studies linking human Siglec-XII expression to pathophysiology and clinical implications are still limited. Recent findings have implicated the aberrant expression of Siglec-XII to oncogenesis and tumour progression [15,23]. These studies have opened a potentially new horizon to explore the potency and efficacy of using targeted immunotherapy for treating RC with Siglec-XII neoantigens. Although, some studies have researched the role of *SIGLEC12* in cancer development, to the best of our knowledge this is the first study assessing the clinical utility and role of *SIGLEC12* in RC using multiomics datasets.

In this study, we investigated Siglec-XII expression in RC and normal tissue, identified oncogenic pathways upregulated in RC expressing *SIGLEC12*, analysed the impact of immune cell infiltration on targeted immunotherapy and addressed the predictive value of *SIGLEC12* and the communication with other genes in RC cohorts.

2. Materials and methods

2.1. The Human Protein Atlas

SIGLEC12 mRNA expression level was analysed in RC and matched normal tissues using data from The Human Protein Atlas (www.proteinatlas.org accessed on January 04, 2023) [24]. For this purpose, we applied filters for the gene *SIGLEC12* and selected pathology as RC. Additionally, we queried kidney single-cell specificity for macrophage clustering using the Single-cell transcriptomics datasets (GSE131685). Tissue RNA was searched for expression clustering and correlation with cluster 64 information. The Human Protein Atlas datasets are accessible via this link: <https://www.proteinatlas.org/ENSG00000254521-SIGLEC12> (accessed on January 04, 2023).

2.1.1. Ualcan

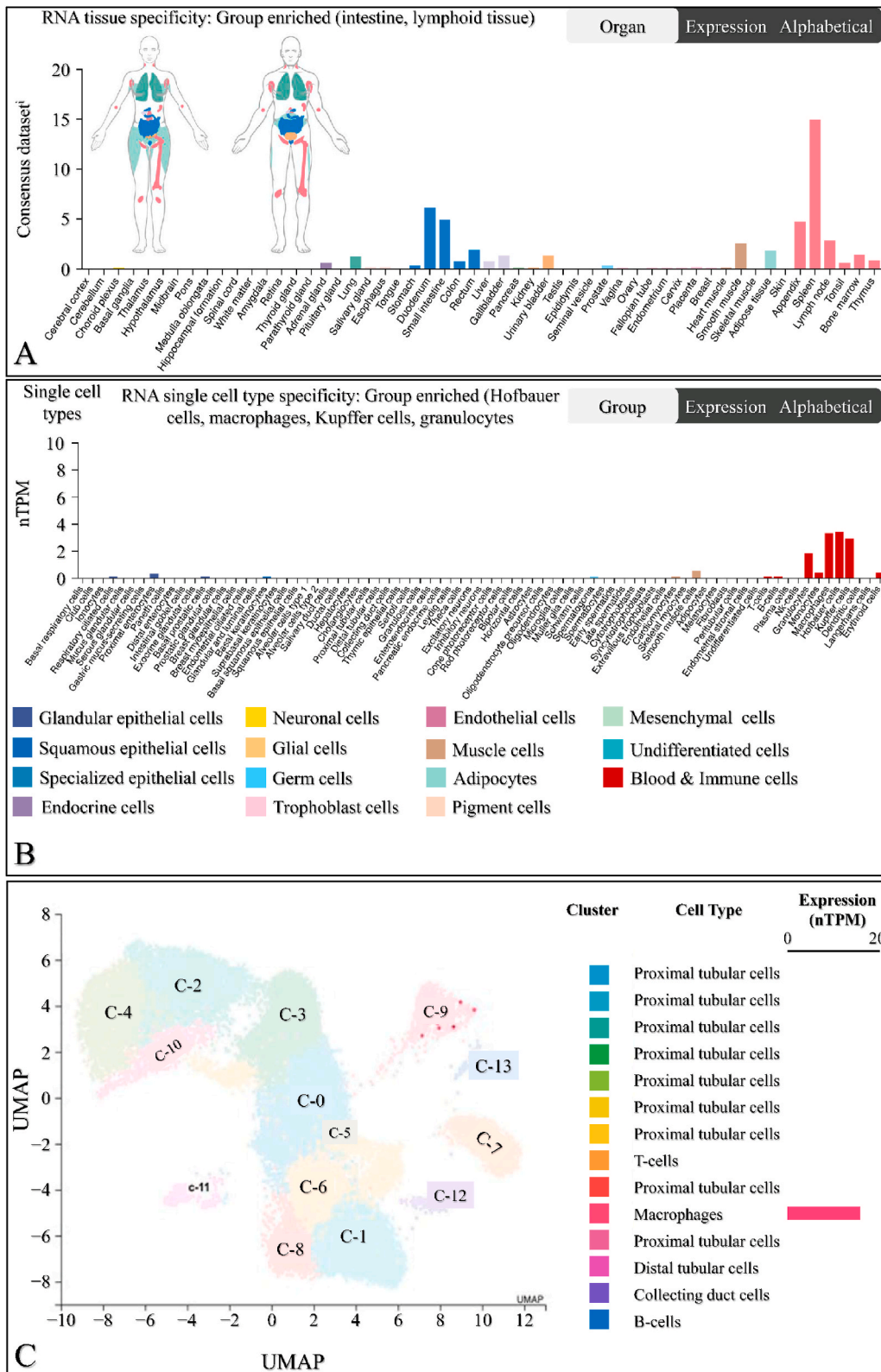
The online data tool UALCAN (<http://ualcan.path.uab.edu> accessed on January 04, 2023) [25] is used to illustrate, analyse, and integrate data from cancer transcriptomics. We compared the expression and methylation levels of *SIGLEC12* in different subgroups of RC using TCGA (The Cancer Genome Atlas) setpoints. Furthermore, we explored the PanCancer studies across the TCGA. The TCGA dataset is available via the following link: <https://portal.gdc.cancer.gov/> accessed on January 04, 2023 (Ensembl: ENSG00000254521).

2.1.2. Identification of miRNA and Venn diagram

To predict target miRNAs associated with *SIGLEC12*, we employed three databases. (1) TargetScan (https://www.targetscan.org/vert_80/ accessed on September 08, 2023), this algorithm predicts miRNA targets across multiple genomes [26,27]. miRWalk (<http://mirwalk.umm.uni-heidelberg.de>, accessed on September 08, 2023), is a Perl-based system that uses computational approach to predict target sites [28]. (2) miRSystem (<http://mirsystem.cgm.ntu.edu.tw>, September 08, 2023) is a web-based tool, that converts queried miRNAs to the latest annotation and integrates miRNA target pathways with gene predictions [29]. The miRNA datasets obtained from all three systems were visualized using Venny (3). The miRNA datasets obtained from all three systems were visualized using Venny (v.2.1; <https://bioinfogp.cnb.csic.es/tools/venny/> accessed on September 08, 2023). Venny is a tool that visually represents the miRNA genes from different databases in the form of a Venn diagram [30].

2.1.3. Kaplan-Meier plotter

Using the Kaplan–Meier plotter (KM plotter) (<https://kmplot.com/analysis> accessed on January 04, 2023), [26,27] to explore the prognostic significance of *SIGLEC12* expression in different subtypes of RC. Furthermore, we conducted an analysis of the mutation burden and macrophage effect in the overall survival (OS) of patients, considering specific categories as part of the restricted analysis subtypes. The datasets used in the KM plotter analysis were sourced from the TCGA datasets, specifically KIRC and KIRP. For more information on the TCGA cancers included in our study, please refer to the following link: <https://www.cancer.gov/about-nci/organization/ccg/research/structural-genomics/tcga/studied-cancers> (accessed on January 04, 2023)



(caption on next page)

Fig. 1. The RNA expression of SIGLEC12 in normal human tissue and the kidney. The expression of SIGLEC12 in different body tissue derived from the Human Protein Atlas; Representation of SIGLEC12 in different human tissue, male (right) and female (left) with the respective distribution according to tissue specificity showed high RNA expression in intestine, lung, liver, lymphoid tissue, and smooth muscle cells (A). Immune cells such as macrophages, Kupffer cells, granulocytes and Hoffbauer cells are RNA grouped enriched Siglec-XII cells (B). High RNA expression of SIGLEC12 in kidney seen in macrophages clusters (12.9 nTPM at 699 cell count) (C).

2.1.4. Tumor Immune Estimation Resource (TIMER) analysis

Online tool TIMER (<https://cistrome.shinyapps.io/timer/> accessed on January 04, 2023) [28] to access the correlation between mRNA expression of the SIGLEC12 gene in TCGA RCRC subtypes and parameters such as tumour purity and the infiltration levels of six distinct immune cell types (including B cells, CD4⁺ T cells, CD8⁺ T cells, neutrophils, macrophages and dendritic cells). This analysis involved the evaluation of the KIRC and KIRP datasets, accessible via the following link: <https://cistrome.shinyapps.io/timer/> (accessed on January 04, 2023). Similarly, we investigated the correlation between SIGLEC12 gene expression and immune checkpoint proteins.

2.1.5. cBioPortal and gene set enrichment analysis

The cBioPortal for Cancer Genomics (<http://cbioportal.org/> accessed on January 04, 2023) [29,30] is an open access resource platform for interactive and programmatic exploration of multiomic cancer data. In our analysis, we focused on kidney renal clear cell carcinoma (ccRCC) from the TCGA PanCancer Atlas, comprising 512 samples. We accessed this dataset through the following link: https://www.cbioportal.org/results?cancer_study_list=kirc_tcg_pan_can_atlas_2018&tab_index=tab_visualize&case_set_id=kirc_tcg_pan_can_atlas_2018_all&Action=Submit&gene_list=SIGLEC12. Our query initially targeted SIGLEC12, and we subsequently refined it to consider mRNA expression relative to normal samples. Subsequently, we downloaded the mRNA comparison and survival data (Human Gene Set: KEGG_RENAL_CELL_CARCINOMA) for further analysis. This analysis was conducted using the Gene Set Enrichment analysis (GSEA) software available at (<https://www.gsea-msigdb.org/> accessed on January 04, 2023) [31], a tool that associates disease phenotypes with groups of genes/proteins represented in a quantitative expression data.

2.1.6. Gene ontology (GO) and kyoto Encyclopaedia of genes and genomes (KEGG) analysis

Furthermore, we also conducted a comparative analysis of GO pathways and KEGG pathways (<http://cbioportal.org/> accessed on September 08, 2023) [29,30]. In this analysis, we performed a search for mRNA expression and obtained data related to SIGLEC12 for ontology categories such as cellular component, biological process, molecular function, and KEGG pathway enrichment. The data sources used for this analysis are available at [32,33].

2.1.7. GeneMania

We identified the functional interactions of SIGLEC12 with hub-bottlenecks genes, those with the highest degree and betweenness centrality values, using the GeneMania database (<https://genemania.org> accessed on January 04, 2023) [34]. This research database provides valuable insights into interaction relationships within the analysed network. We specifically queried hub-bottlenecks for each experimental category, including physical interaction and co-expression, related to SIGLEC12. The GeneMania database can be accessed via the following link: <https://genemania.org/search/homo-sapiens/siglec12> (Last database update: August 13, 2021, Application version: 3.6.0, accessed on January 04, 2023).

2.1.8. STRING pathway

For the integration of additional protein-protein interactions (PPIs), we utilized the STRING search tool (<https://string-db.org> accessed on September 08, 2023). This comprehensive database encompasses approximately 9,600,567 proteins from 2024 organisms and 933,668,678 PPIs [35,36]. (9,10). We initiated a protein search by name for SIGLEC12 and applied additional filters to retrieve more PPIs predictions.

2.1.9. Statistical analyses

All statistical methods, data, and statistical values were directly obtained from the corresponding database. The Kaplan-Meier survival plots, including the of individuals, instantaneous event rate, hazard ratio (HR), 95 % confidence intervals (CI), and log-rank *P*-values, were extracted from the respective databases. For GSEA, we considered *P*-values ≤ 0.05 and false discovery rate (FDR) *q*-value ≤ 0.25 as statistically significant. A *P*-values of ≤ 0.05 was used as the threshold for statistical significance. The levels of significance were denoted as **p* ≤ 0.05 , ***p* < 0.01 , ****p* < 0.001 , *****p* < 0.0001 .

3. Results

3.1. SIGLEC12 is expressed in human body tissue

The mRNA expression of SIGLEC12 in different tissue types was analysed using the Human Protein Atlas database. Tissue specificity was compared across various tissue types. The results showed that the mean values of SIGLEC12 expression in tissues are as follows: intestine (2.78 consensus normalized transcript expression, nTPM), lung (2.2 nTPM), liver (0.7 nTPM), lymphoid tissue (4.2 nTPM), and smooth muscle (2.5 nTPM) (Fig. 1A). The single-cell specificity results indicated that immune cells, such as macrophages, Kupffer

cells, granulocytes, and Hoffbauer cells, are enriched in *SIGLEC12* (Fig. 1B). Within the kidney immune cells, the level of *SIGLEC12* expression showed high RNA expression in macrophage clusters, with 12.9 nTPM at 699 cell count (Fig. 1C). These results suggested that macrophage-specific *SIGLEC12* expression is a major contributor to *SIGLEC12* expression in renal tissue.

3.2. *SIGLEC12* is expressed in other types of cancer

We aimed to elucidate the PanCancer profile of *SIGLEC12* expression in The Cancer Genome Atlas (TCGA) using the UALCAN tool. *SIGLEC12* expression was found to be upregulated in bladder urothelial carcinoma (BLCA), cervical squamous cell carcinoma (CESC), esophageal carcinoma (ESCA), and Glioblastoma multiforme tumours (GBM) when compared to the normal sample type (Fig. 2). In contrast, colon adenocarcinoma (COAD), lung adenocarcinoma (LUAD), lung squamous cell adenocarcinoma (LUSC), and pancreatic adenocarcinoma (PAAD) exhibited downregulation of *SIGLEC12* when compared to healthy samples (Fig. 2).

3.3. Increased expression of *SIGLEC12* correlates with primary tumour growth in renal cancer

By using UALCAN, we compared *SIGLEC12* expression in KIRC and normal tissue sample (Fig. 3A). Similarly, we compared the expression of *SIGLEC12* in KIRP with the normal sample type (Fig. 3B). Both results showed a statistically significant increase in the expression of *SIGLEC12* in primary tumour. To understand gender related *SIGLEC12* expression in tumour development (Fig. 3C–D), we compared normal sample type with males, the normal sample type with females and both genders. There was a statistically significant increase between normal sample types when compared with different gender in both cancer types (Fig. 3C–D). However, there was no correlation between the level of *SIGLEC12* expression and genders (KIRC $p = 0.91$ Fig. 2C, KIRP $p = 0.91$ Fig. 3D). Moreover, we investigated *SIGLEC12* expression versus age distribution in the cancer subsets (Fig. 3E–F). No statistically significance difference in the expression of *SIGLEC12* was observed for patients aged 21–40years in KIRC ($p = 0.3$) (Fig. 3E), and for patients 81–100years in KIRP was observed ($p = 0.12$), Fig. 3F). Other age group distributions showed a statistical increase in *SIGLEC12* expression. Furthermore, we analysed the effect of *SIGLEC12* expression on the cancer stage (Fig. 3G–H), and the results showed an increase in tumour progression for all stages except for KIRP individuals ($p = 0.8$), (Fig. 3H). We further elucidated the significance of *SIGLEC12* expression in tumour nodal metastasis, result showed a statistically significant increase in the metastases according to the tumour, node, metastasis (TNM) staging framework, N0 in KIRC (Fig. 3I) and N0, N1, N2 in KIRP (Fig. 3J).

3.4. Increased miRNA mediated regulation in *SIGLEC12* expression of *SIGLEC12* correlates with primary tumour growth in renal cancer

We utilized three multi-omics databases: TargetScan, miRsystem, and miRwalk, to investigate the impact of miRNA on *SIGLEC12* expression. These databases are user-friendly tools for predicting loci that match biological targets, target genes, associated pathways, and miRNA binding sites, respectively. The results, represented in a Venn diagram, suggest an overlap of six (6) miRNAs common to all

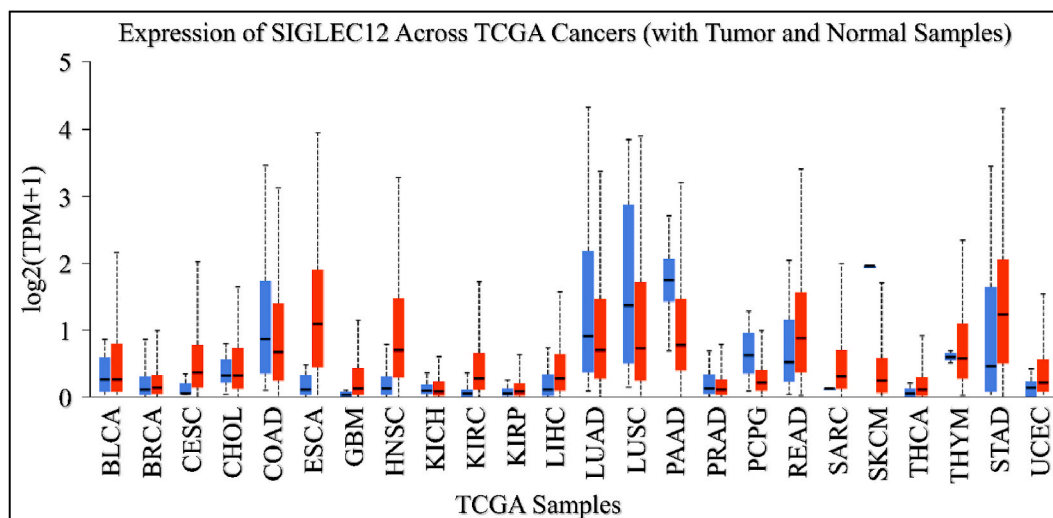


Fig. 2. The PanCancer studies revealed both upregulation and downregulation of *SIGLEC12* expression across various tumour types. Key- bladder urothelial carcinoma (BLCA), breast invasive carcinoma tumour (BRCA), cervical squamous cell carcinoma (CESC), cholangiocarcinoma (CHOL), colon adenocarcinoma (COAD), esophageal carcinoma (ESCA), glioblastoma multiforme (GBM), head and neck squamous cell carcinoma (HNSC), kidney chromophobe (KICH), kidney renal clear cell carcinoma (KIRC), liver hepatocellular carcinoma (LIHC), lung adenocarcinoma (LUAD), lung squamous cell adenocarcinoma (LUSC), pancreatic adenocarcinoma (PAAD), prostate adenocarcinoma (PRAD), pheochromocytoma and paraganglioma (PCPG), rectal adenocarcinoma (READ), sarcoma (SARC), skin cutaneous melanoma (SKCM), thyroid carcinoma (THCA), thymoma (THYM), stomach adenocarcinoma (STAD) and uterine corpus endometrial carcinoma (UCEC).

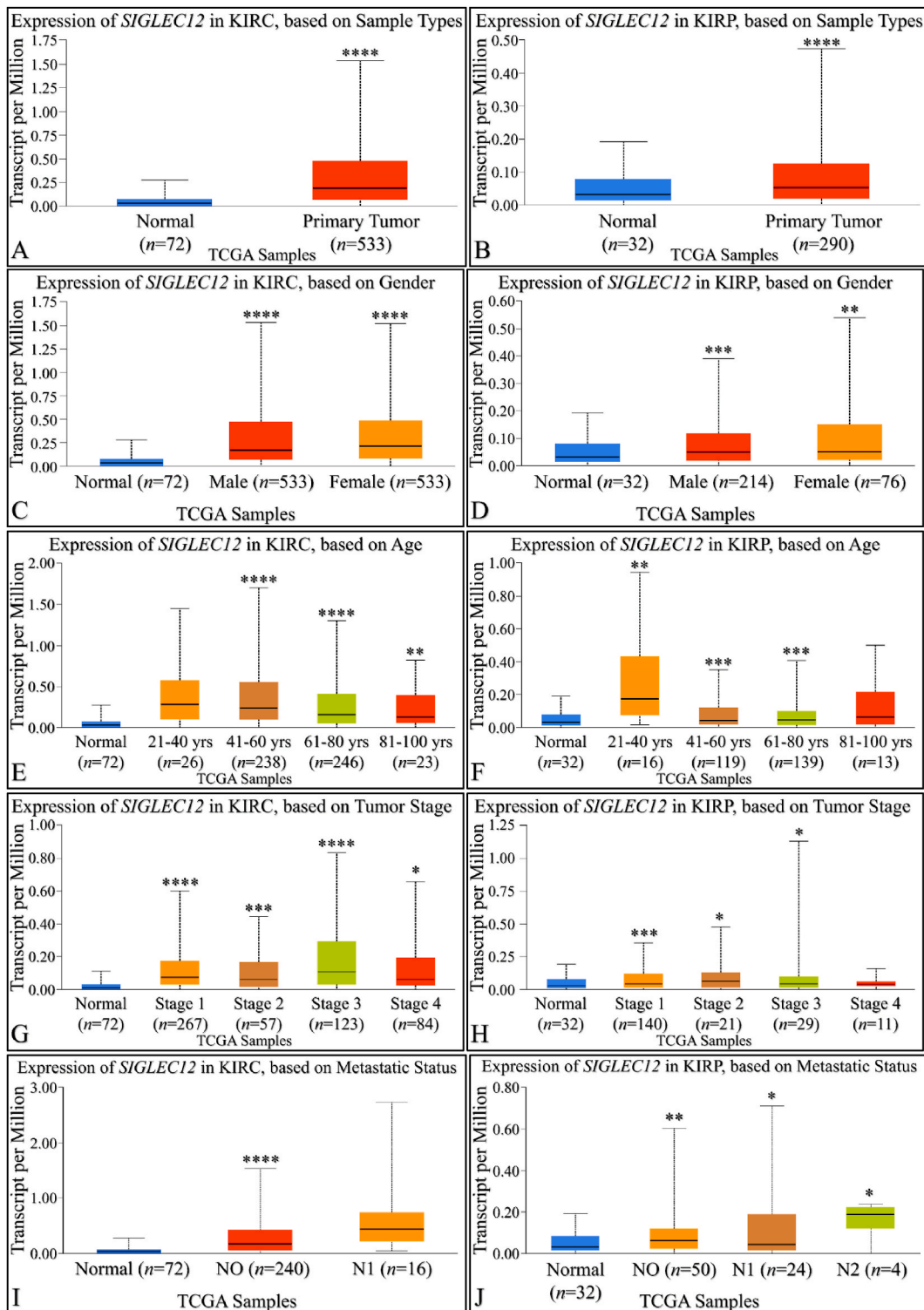


Fig. 3. *SIGLEC12* expression in sample types. Primary tumour in KIRC patient's vs normal (**** $p < 0.0001$) (A). Primary tumours in KIRP vs normal sample types (**** $p < 0.0001$) (B). Expression of *SIGLEC12* in KIRC based on Patient's gender (C). Expression of *SIGLEC12* in KIRP based on Patient's gender (E) Expression of *SIGLEC12* in KIRC based on Patient's age (D). Expression of *SIGLEC12* in KIRP based on Patient's age (F). Expression of *SIGLEC12* in KIRC based on individual cancer stages (G). Expression of *SIGLEC12* in KIRP based on individual cancer stages (H). Expression of *SIGLEC12* in KIRC based on nodal metastases status (I). Expression of *SIGLEC12* in KIRP based on nodal metastases status (J). The level of significance indicated as * $p < 0.05$, ** $p < 0.01$, *** $p < 0.001$, **** $p < 0.0001$.

three databases associated with *SIGLEC12* (Fig. 4A and G). These miRNAs are hsa-miR-133b, hsa-miR-654-5p, hsa-miR-574-5p, hsa-miR-663a, hsa-miR-541-3p, and hsa-miR-371a-5p. To gain a deeper understanding of the impact of these miRNAs on the upregulation and downregulation of protein synthesis in KIRC and KIRP, we conducted a search for each of the six (6) common miRNAs using the UALCAN tool. In KIRC, the results showed statistically significant upregulation of miRNA in Fig. 4B and C. Conversely, Fig. 4D demonstrated statistically significant downregulation. The miRNA expression in Fig. 4E and F was not statistically significant (NS), with p -values of 0.29 and 0.38, respectively. In KIRP, the results indicated statistically significant upregulation of miRNA in Fig. 4H and I, J, and 4L. However, the miRNA expression in Fig. 4K was not statistically significant (NS) with a p -value of 0.5. These results may influence the protein synthesis of *SIGLEC12*-related tumours.

3.5. Multivariate analysis of overall survival (OS) and relapse free survival (RFS) of *SIGLEC12* using KM plotter

The database contains gene expression profiles and survival data for PanCancer analysis. We validated the association between the expression levels of *SIGLEC12* and overall survival rate in RC (Fig. 5A–B). High *SIGLEC12* mRNA expression in KIRC (HR = 1.51; 95% CI: 1.12–2.05; $P < 0.0069$), (Fig. 3A), and KIRP (HR = 2.03; 95%CI: 1.1–3.73; $P < 0.02$), (Fig. 5B), was significantly associated with

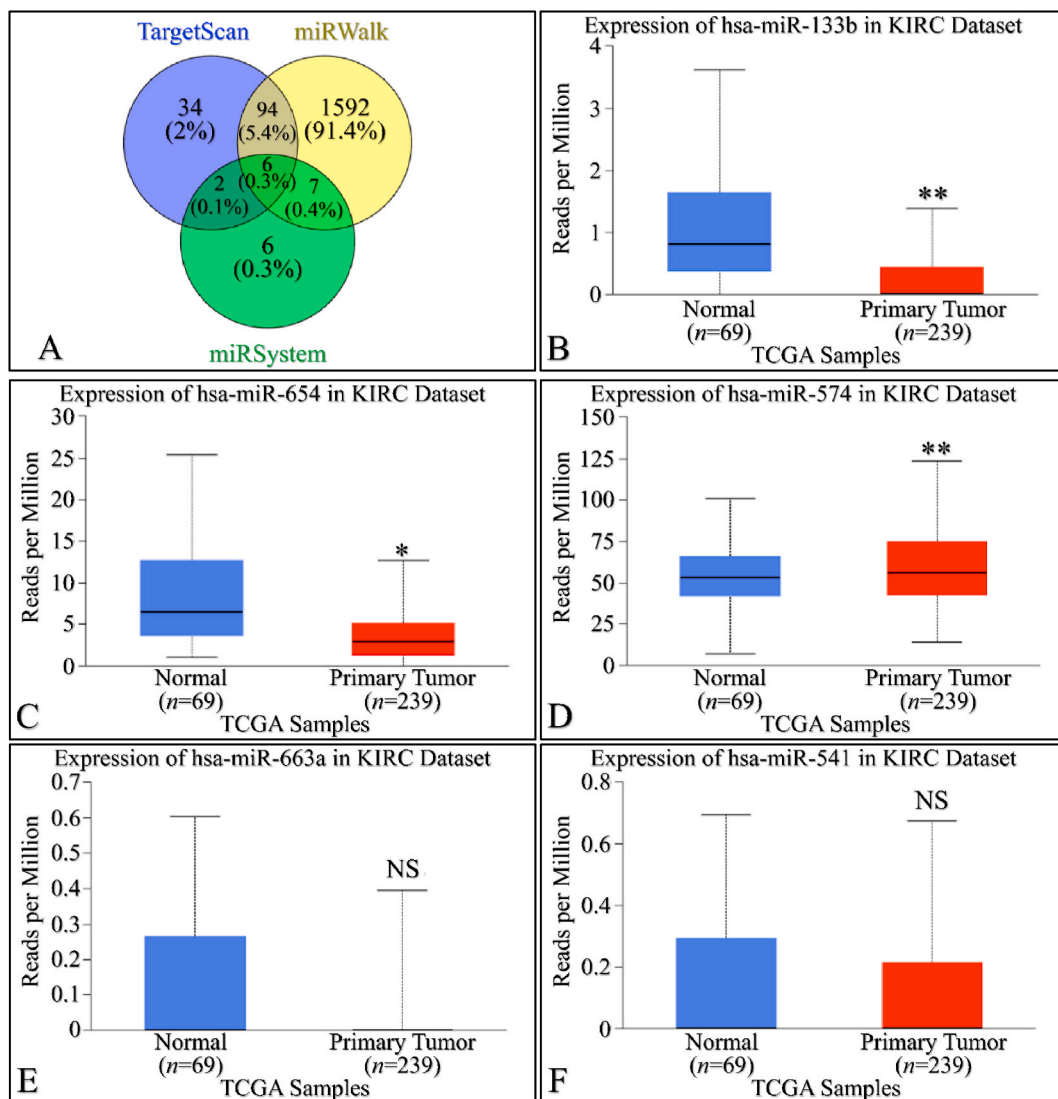


Fig. 4. MiRNA expression of *SIGLEC12* in RC. The results of the miRNA expression showed upregulation and downregulation of miRNA. Venn diagram showing all three data bases (A and G), expression of hsa-miR-133b in KIRC (B), expression of hsa-miR-654-5p in KIRC (C), expression of hsa-miR-574-5p in KIRC (D), expression of hsa-miR-663a in KIRC (E), expression of hsa-miR-541-3p in KIRC (F), expression of hsa-miR-133b in KIRP (H), expression of hsa-miR-654-5p in KIRP (I), expression of hsa-miR-574-5p in KIRP (J), expression of hsa-miR-663a in KIRP (K) and expression of hsa-miR-541-3p in KIRP (L).

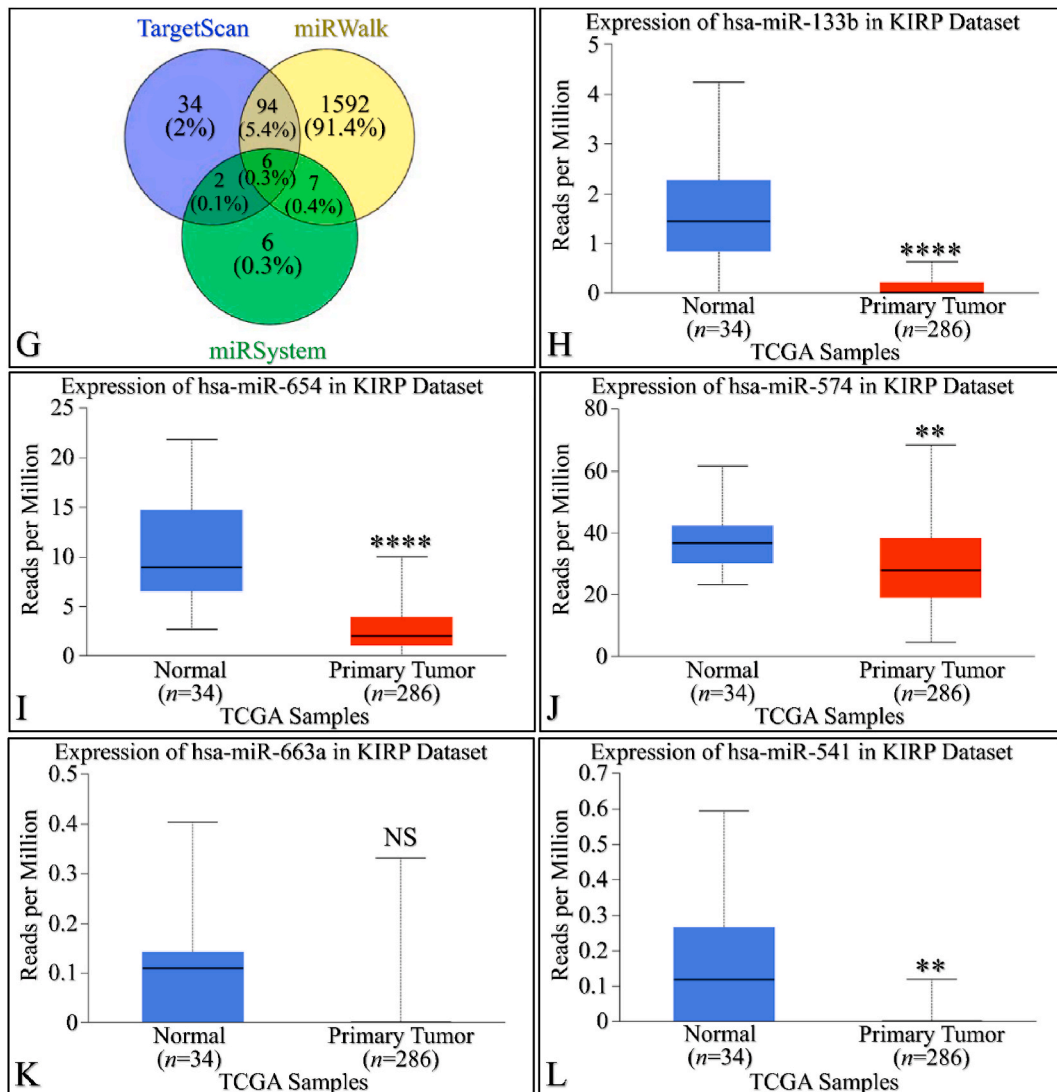


Fig. 4. (continued).

worse OS. Data for RFS indicates that there was no correlation in the expression levels of *SIGLEC12* and RFS for KIRC (HR = 2.22; 95% CI: 0.62–7.95), (Fig. 5C). However, KIRP suggested a statistically significant increase in the survival of low expression cohorts (Fig. 5D). The high mutation burden of *SIGLEC12* resulted in the worst patient outcome for KIRC (HR = 1.84; 95%CI: 1.05–3.24; $P < 0.032$), (Fig. 5E), while there was no correlation between mutation in *SIGLEC12* and KIRC patients' survival (HR = 1.75; 95%CI: 0.63–4.83; $P < 0.27$), (Fig. 5F). Enhanced macrophage infiltration is associated with worse prognosis in KIRC (HR = 1.49; 95%CI: 1.07–2.08; $P < 0.017$) (Fig. 5G), and KIRP (HR = 2.25; 95%CI: 1.12–4.53; $P < 0.02$), (Fig. 5H).

3.6. Association of *SIGLEC12* expression with immune cell infiltration in tumour-immune microenvironment

The TIMER online tool evaluates immune infiltration based on a predetermined signature gene matrix of the immune subsets (11). In KIRC, this analysis revealed a clear weak negative correlation of *SIGLEC12* with tumour purity ($r = -0.156$, $p < 0.0007$), (fig. 6A1). A partial correlation in the abundance of tumour-infiltrating immune cells such as CD8⁺T cells (Fig. 6A5), CD4⁺ T cells (Fig. 6A7), macrophages (Fig. 6A9), neutrophils (Fig. 6A11), and dendritic cells (Fig. 6A13) was noted in KIRC (Fig. 6A upper row). B-cell infiltrations suggested no correlation (Fig. 6A3).

In KIRP, the tumour purity data suggested no correlation ($\rho = -0.081$, $p = 0.1$) (Fig. 6A2). However, a partial correlation in the abundance of tumour-infiltrating immune cells such as B-cells (Fig. 6A4), CD8⁺ T cells (Fig. 6A6), neutrophils (Fig. 6A12), and dendritic cells (Fig. 6A14) was observed. CD4⁺ T cells (Fig. 6A8) manifested a higher correlation coefficient compared to CD8⁺ T cells. Interestingly, there was no correlation in macrophage infiltration (Fig. 6A10). Furthermore, in *SIGLEC12* KIRC we observed no

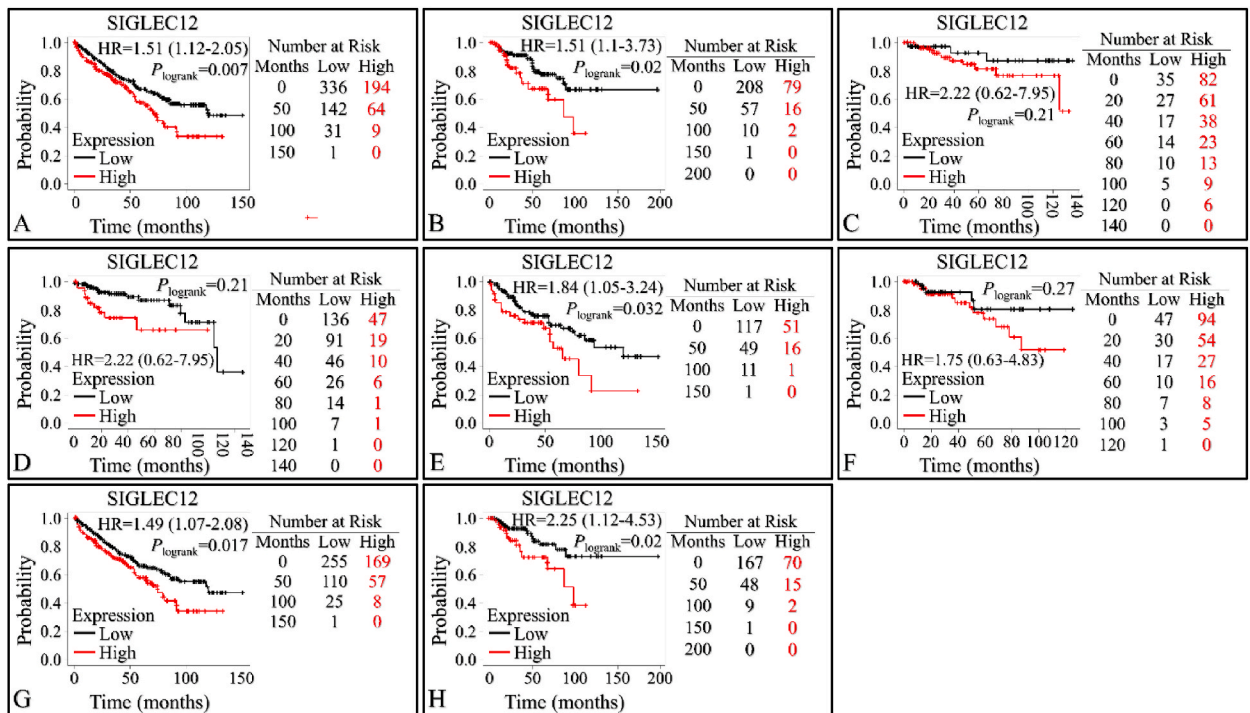


Fig. 5. Prognosis value of *SIGLEC12* OS and RFS according to KM plotter. OS of *SIGLEC12* mRNA expression in KIRC (A). OS of *SIGLEC12* mRNA expression in KIRP (B). RFS of *SIGLEC12* mRNA expression in KIRC (C). RFS of *SIGLEC12* mRNA expression in KIRP (D). Mutation burden in KIRC (E). Mutation burden in KIRP (F). Enriched macrophage expression in KIRC (G). Enriched macrophage expression in KIRP (H).

correlation in immune checkpoint proteins PDCD1 (PD-1) (Fig. 6B1), while CD274 (PDL-1) (Fig. 6B), CTLA4 (Fig. 6B3), IL-2 (Fig. 6B4) had a weak positive correlation. Similarly, in KIRP *SIGLEC12* positive tumours, a weak positive correlation in PDCD1 (Fig. 4C1), CD274 (Fig. 6C2), CTLA4 (Fig. 6C3), IL-2 (Fig. 6C4) was observed.

3.7. Enrichment of gene phenotype and biological pathways

We investigated *SIGLEC12* mRNA expression using transcriptome correlation analysis of TCGA ccRCC in cBioportal web server. Furthermore, to pinpoint the biological pathways in which the *SIGLEC12* associated genes were enriched, we applied the GSEA analysis. Our results suggested that the hallmark of gene pathways significantly enriched and positively correlated with *SIGLEC12* expression are interferon gamma (IFN- γ) response, interleukin 2 signal transducer and activator of transcription 3 (IL-2_STAT3), tumour necrosis factor (TNF)- signalling via nuclear factor kappa B (NF- κ B), KRAS, and IL6_JAK-STAT3 signalling (Fig. 7A-H), Table 1. While the correlation in mammalian target of rapamycin complex 1 (MTORC1), Phosphoinositide 3-kinases_Protein kinase B_MTOR (P13K_AKT_MTOR), transforming growth factor β (TGF- β) was not statistically significant (Fig. 7I-L), Table 1.

3.8. GO and KEGG analyses

We further investigated other mRNA targeted expression impacting the enrichment pathways of *SIGLEC12* on cBioportal. The outcome suggests that 33 % of the of *SIGLEC12*-associated pathways have high mRNA expression compared to healthy individuals. Additionally, we collated only the significant mRNA survival data and queried it for Homo sapiens in the STRING database. We then analysed the data for enrichment KEGG (Fig. 8A) enrichment process (Fig. 8B) enrichment function (Fig. 8C) and enrichment component (Fig. 8D). The results suggested that different pathways may be upregulated or downregulated in *SIGLEC12* mRNA expression.

3.9. *SIGLEC12* communicates with genes implicated in cancer development

To explore the possibility of *SIGLEC12* communication with other genes, and the effect of this communication in carcinogenesis, we used the GeneMANIA tool and searched for *SIGLEC12*. *SIGLEC12* revealed a series of gene co-operators and interactions (Fig. 9A). We analysed two basic features: *SIGLEC12* physical interactions (Fig. 9B) and co-expression (Fig. 9C) with other genes. The physical interaction (77.64 %) revealed *SIGLEC12* linkage with TEX261, MIA3 and PLAA genes with TEX261 exerting the strongest interaction

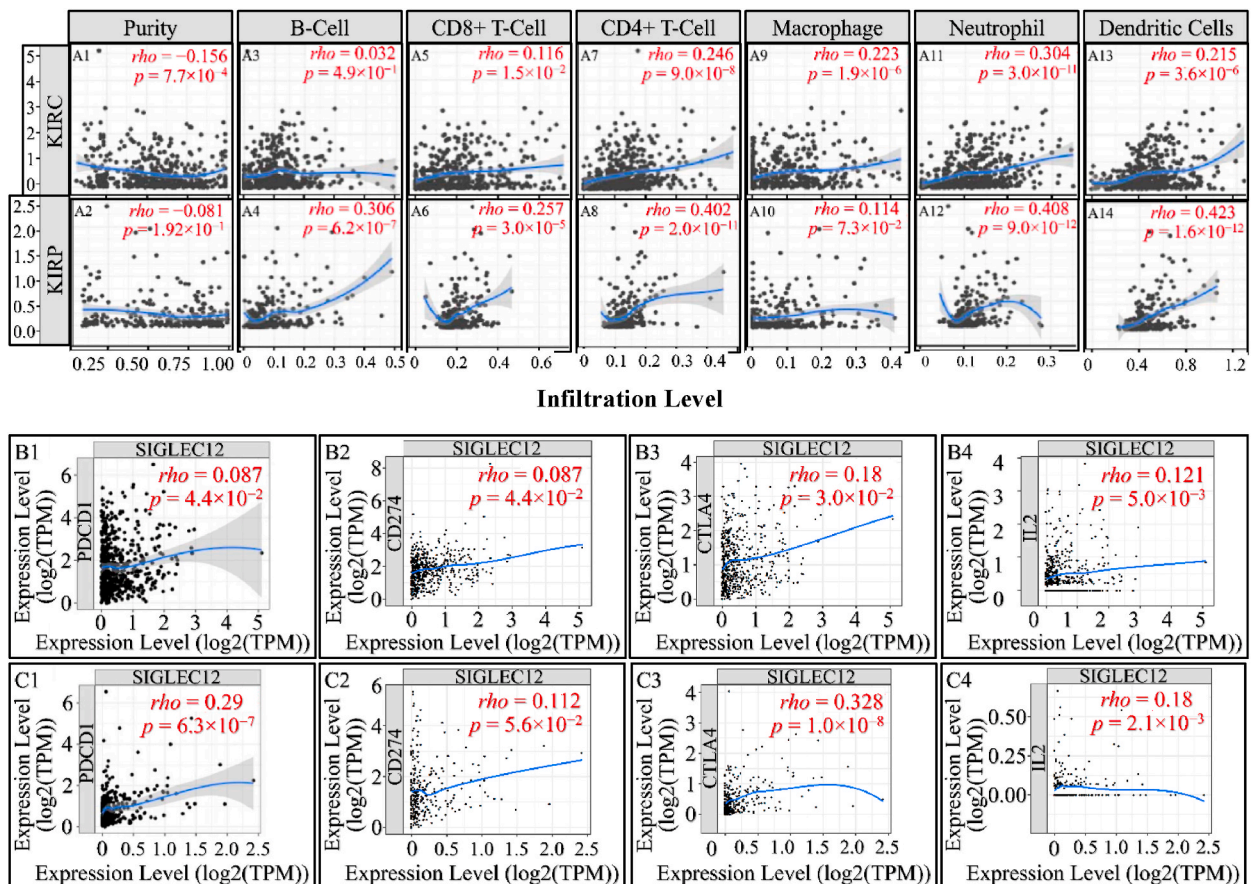


Fig. 6. Association of *SIGLEC12* expression with the tumour-immune microenvironment. Scatter plots representing the association of *SIGLEC12* expression with the tumour-immune microenvironment using TIMER (A1–A14). Spearman correlation analysis of *SIGLEC12* with immune checkpoint protein such as PD-1, PDL-1, CTLA4 and IL-2 in KIRC (B1–B4). Correlation of *SIGLEC12* with immune checkpoint proteins such as PDCD1, CD274, CTLA4 and IL-2 in KIRP (C1–C4).

(Fig. 9B). Similarly, Fig. 9C describes a potential mechanism of co-expression with hub of several genes.

To improve the robustness and understand the functional associations of the data gathered from GeneMANIA, we decided to compare the data with STRING. The result suggested that genes such as *TEX261* and *MIA3* were common to Fig. 9A–C and Fig. 9D databases. Furthermore, Fig. 9D showed a high level of physical interaction among *MIA2*, *Siglec1*, *Siglec15* and Eukaryotic initiation factor (EIF) subgroups.

4. Discussion

In the present study, we comparatively analysed the significance of the expression of *SIGLEC12* mRNA in normal tissue. In previous studies, authors have shown that there is epithelial expression of Siglec-12 in all chimpanzees and Siglec-XII in some human epithelia [15]. We identified that *SIGLEC12* is synchronously expressed only by immune cells such as macrophages. This immune infiltration has been implicated as an important stromal element in TME [37]. Importantly, macrophages function as an antigen presenting cell (APCs) by activating other innate and adaptive immune cells through various autocrine and paracrine mediated pathways [38,39]. This finding collaborates Mitra et al. (2011) [17] conclusion that macrophage express Siglec-12 in the prostate, kidney, stomach, and pancreas of chimpanzees. In contrast, we could not detect Siglec-XII in epithelia cells. We could attribute this inconsistency to the potential limitations of our current tools' sensitivity to the subject matter. However, despite our tool's bias, we believe that Siglec-XII is expressed in human epithelia cells. This is also consistent with Mitra et al. (2011) [17]. To reemphasize, it is still unclear from this result, whether the high expression of *SIGLEC12* seen in secondary lymphoid organs and other tissues may result in the possibility of high *SIGLEC12* related tumour prevalence in these tissues.

Furthermore, our results suggested that *SIGLEC12* associated RC prevalence is not gender based. Also, the increase in primary tumour subtypes indicated that Siglec-XII expression may play a role in RC development. This proposition is consistent with previous findings in mice, where human prostate cancer cells transfected with human *SIGLEC12* showed significant tumour growth when compared with non-expressing cells over a 70-day period [17]. The finding that the effect of *SIGLEC12* on RC may not be related to the

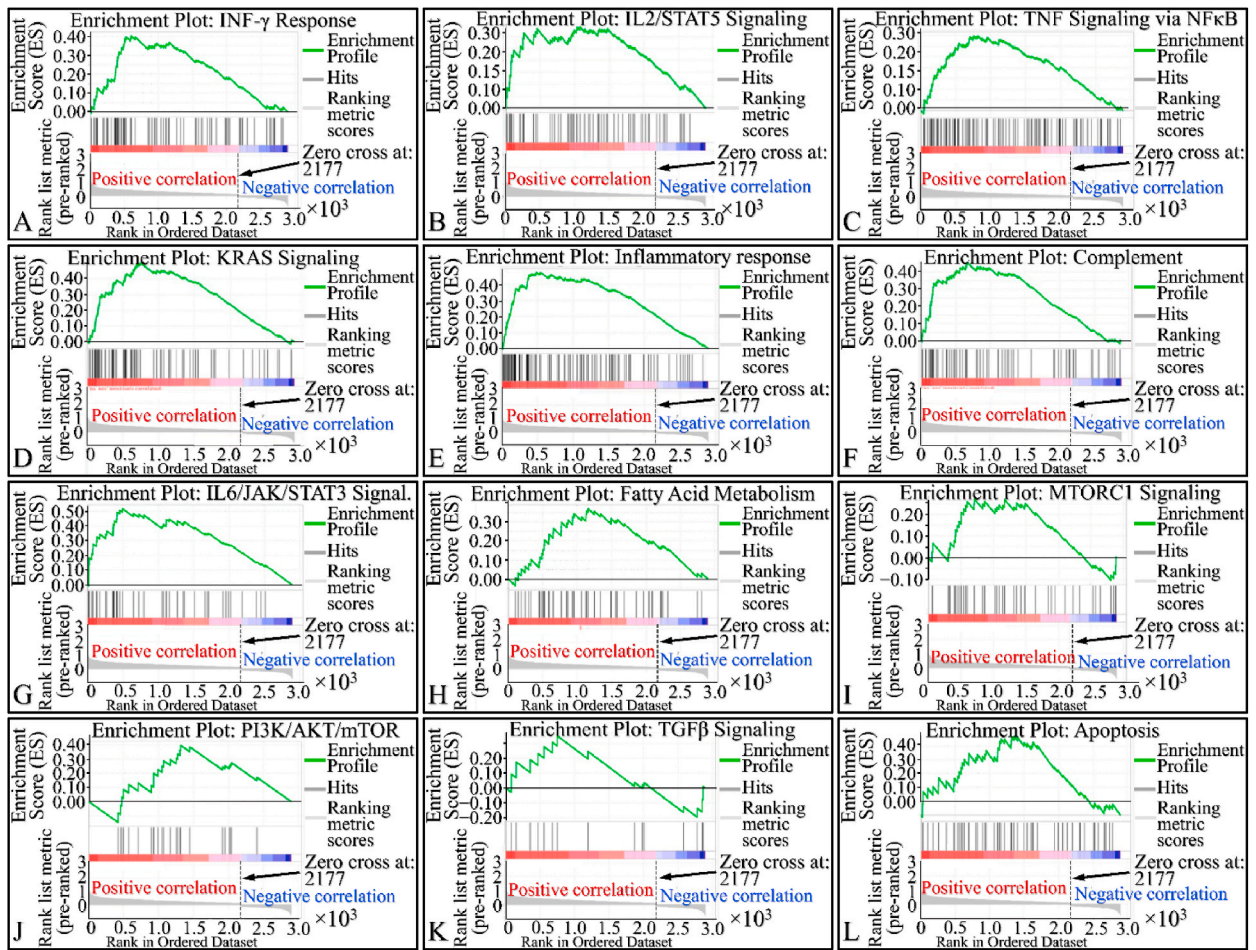


Fig. 7. Enrichment of gene phenotype and biological pathways. Gene set enrichment analysis of *SIGLEC12* co-expression gene profile in ccRC (A–L) using GSEA. Subfigures A–H present statistically significant annotations. Subfigures I–L present not statistically significant annotations (Legend: NES: Normalized Enrichment Score, FDR: False Discovery Rate).

age of the patient led to the suggestion that even in paediatrics RC, these cancers might occur in a similar manner. Furthermore, the results from the cancer stages and nodal metastasis showed clinical relevance in the staging of these cancer needs to be further investigated. It is theoretically possible that the observed effects could vary based on the amount of Siglec-XII or immune cell infiltration. These expressions may have a long-term effect on the progression of cancer and eventual disease severity. To reiterate, it has been established that different immune cells inter-react vigorously to promote or inhibit tumour progression in the TME [15,40]. If a relation between the grade and stage of the tumour can be validated and consistent, it can become a potential prognostic tool. Indeed, Esserman et al. (2009) observed that in early-stage prostate cancer most patients may develop microscopic disease with advancing age, and only a minority may result in metastatic disease [41]. Similarly, the expression of *SIGLEC12* across the TCGA cancers reinforces the proposition that some cancer may have the *SIGLEC12* gene as part of other gene responsible for their tumour formation.

Advances in transcriptomes studies and high-throughput systems have continually unravelled the bottlenecks in the complexity of the RNA dogma [42]. MiRNAs are a classes of short non-coding RNAs (ncRNAs) that bind to mRNA, which later forms the template for protein synthesis [42,43]. The binding of miRNA to a specific 3' untranslated region of mRNA could result in the inhibition of translating mRNA to proteins [43]. The available data has shown that hsa-miR-133b and hsa-miR-663a miRNAs may be upregulated in Siglec-XII expressing RC. Liu et al. (2020) [43] noted that hsa-miR-133b are downregulated in carcinoma of the lung, which also reinforces our initial PanCancer study. Furthermore, in KIRC, hsa-miR-574-5p is downregulated, while in KIRP, it is upregulated. The difference between the two databases is a limitation why the latter was upregulated in KIRP and downregulated in KIRC. We also propose that hsa-miR-371a-5p has no role in transcriptomics dogma of Siglec-XII expressing RC. To point out, although the small size of our normal sample may pose a significant bias and imprecision to our postulations, we still believe that these miRNAs could be playing a role in the progression or repression of RC *SIGLEC12* gene expression.

We demonstrated the essential features of the KM plotter survival probability. At first glance, *SIGLEC12* showed high expression in most descriptors, which resulted in a poor patient outcome. However, some descriptors mentioned earlier were not statistically significant. Indeed, the overall findings suggested that deleterious mutations, oncogenic pathways, and enzymes might be upregulated by

Table 1Gene enrichment for hallmark genes. The level of significance indicated as * $p < 0.05$, ** $p < 0.01$, *** $p < 0.001$, **** $p < 0.0001$ at a FDR<0.25 level.

Inv.	Gene sets enrichment	Nominal p -value	FDR (q -value)	Leading Edge
1	HALLMARK KRAS SIGNALING UP	0.000	0.000	tags = 60 %, list = 26 %, signal = 78 %
2	HALLMARK INFLAMMATORY RESPONSE	0.000	0.000	tags = 43 %, list = 17 %, signal = 49 %
3	HALLMARK IL6 JAK-STAT3 SIGNA	0.000	0.000	tags = 46 %, list = 17 %, signal = 54%
4	HALLMARK COMPLEMENT	0.000	0.004	tags = 48 %, list = 23 %, signal = 60 %
5	HALLMARK ALLOGRAFT REJECTION	0.000	0.003	tags-67 %, list-39 %, signal-105 %
6	HALLMARK INTERFERON GAMMA RESPONSE	0.000	0.024	tags = 40 %, list = 21 %, signal = 49 %
7	HALLMARK TNFA SIGNALING via NF κ B	0.006	0.104	tags = 42 %, list = 28 %, signal = 56 %
8	HALLMARK APICAL JUNCTION	0.020	0.134	tags = 58%, list = 41 %, signal = 97 %
9	HALLMARK FATTY ACID METABOLISM	0.022	0.155	tags = 59%, list = 40 %, signal = 97 %
10	HALLMARK IL2 STAT5 SIGNALING	0.044	0.213	tags = 48 %, list = 37 %, signal = 75 %
11	HALLMARK PI3K AKT MTOR SIGNALING	0.086	0.252	tags = 71 %, list = 45 %, signal = 129 %
12	HALLMARK OXIDATIVE PHOSPHORYLATION	0.058	0.247	tags = 57%, list = 40 %, signal = 92 %
13	HALLMARK PEROXISOME	0.140	0.283	tags = 43 %, list = 24 %, signal = 56%
14	HALLMARK EPITHELIAL MESENCHYMAL TRANSITION	0.061	0.263	tags = 30 %, list = 19 %, signal = 36 %
15	HALLMARK XENOBIOTIC METABOLISM	0.158	0.372	tags = 51 %, list = 36 %, signal = 79 %
16	HALLMARK COAGULATION	0.300	0.594	tags = 38 %, list = 29 %, signal = 53 %
17	HALLMARK APOPTOSIS	0.256	0.561	tags = 59 %, list = 47 %, signal = 108 %
18	HALLMARK TGF BETA SIGNALING	0.374	0.770	tags = 47 %, list = 26 %, signal = 63 %
19	HALLMARK MTORC1 SIGNALING	0.377	0.736	tags-38 %, list-24 %, signal-49 %
20	HALLMARK ADIPOGENESIS	0.394	0.736	tags = 51 %, list = 41 %, signal = 84 %
21	HALLMARK DNA_REPAIR	0.465	0.792	tags = 33 %, list = 23 %, signal = 43 %
22	HALLMARK ESTROGEN RESPONSE (EARLY)	0.486	0.810	tags = 53 %, list = 46 %, signal = 97 %
23	HALLMARK P53 PATHWAY	0.535	0.841	tags = 65 %, list = 48 %, signal = 123 %
24	HALLMARK HYPOXIA	0.533	0.819	tags = 30 %, list = 25 %, signal = 39 %
25	HALLMARK UV RESPONSE DOWN	0.564	0.788	tags = 51%, list = 46 %, signal = 94 %
26	HALLMARK UV RESPONSE UP	0.546	0.806	tags = 45 %, list = 41 %, signal = 76 %
27	HALLMARK INTERFERON ALPHA RESPONSE	0.569	0.781	tags = 23 %, list = 17 %, signal = 27 %
28	HALLMARK GLYCOLYSIS	0.645	0.847	tags = 66 %, list = 55 %, signal = 143 %
29	HALLMARK BILE ACID METABOLISM	0.621	0.825	tags = 59 %, list = 52 %, signal = 122 %
30	HALLMARK ESTROGEN RESPONSE (LATE)	0.834	1.000	tags = 32 %, list = 31 %, signal = 46 %
31	HALLMARK MYOGENESIS	0.879	1.000	tags = 56 %, list = 51 %, signal = 113 %
32	HALLMARK MITOTIC SPINDLE	0.912	1000	tags = 18 %, list = 16 %, signal = 21 %
33	HALLMARK UNFOLDED PROTEIN RESPONSE	0.908	1.000	tags = 24 %, list = 24 %, signal = 31 %
34	HALLMARK ANDROGEN RESPONSE	0.909	0.979	tags = 25 %, list = 18 %, signal = 30 %
35	HALLMARK KRAS SIGNALING DOWN	0.927	0.958	tags = 52 %,list = 49 %, signal = 100 %
36	HALLMARK REACTIVE OXYGEN SPECIES PATHWAY	0.949	0.961	tags = 53 %, list = 45 %, signal = 96 %

SIGLEC12 in the TME, which associated with poor OS and RFS. It is important to point out that the uneven number of sample size expressing high and low *SIGLEC12* may have contributed to this result. Overall, these findings validate the prognostic value and the relationships between *SIGLEC12*, its mutational burden, and macrophage infiltration in TME. Furthermore, it was reported earlier that KRAS and YAP/TAZ, well-known oncogenic pathways, were enriched in the same manner as the SHP2 pathways [15]. Our analysis validated the former findings that KRAS gene was significantly enriched in the TME [15]. This may suggest that SHP2 recruitment may play an integral path in the oncogenic process in RC. This pathway can trigger the MAPK signalling cascade which has been demonstrated to serve an essential role in cell proliferation, differentiation, development, and metastases of ccRCC [33,34]. Other oncogenic pathways and proteins such as IFN- γ , IL6, and IL2_STAT3 downstream signalling [35] can also be implicated in the deleterious pathways of *SIGLEC12* tumorigenesis and may affect clinical outcomes [36,37].

The double faceted role of IFN- γ , encompassing both anti-tumour and pro tumorigenic effects has been extensively described [44, 45]. The latter effect occurs due to IFN- γ immune evasion and maintaining homeostasis necessary for the thriving of other immunosuppressive cells [44,46]. Preclinical *in vitro* studies have shown that treatment of human melanoma cells with IFN- γ results in growth inhibition. However, it also increases the expression of various tumour markers, including HLA-DR, A.1.43, and -DQ ICAM-1 which are markers in advanced melanomas [46,47]. The suggested correlation between the IFN- γ response and *SIGLEC12* expression is consistent with previous findings demonstrated by Siddiqui et al. (2020) [15]. The complement system consists of a series of proteins that augment the immune and inflammatory response [45]. Earlier we emphasised that *SIGLEC12* is expressed by macrophages, Markiewski et al. (2009) suggested that IgM and IgG, by-products of plasma cells, can bind with tumour antigens to form an antigen-antibody complex, this further results in Fc gamma receptor activation and opsonization with complement 1 (C1), thereby activating the complement system cascade [48]. Reese et al. (2020) suggested that complement proteins recruit and activate immunosuppressive cells in the tumour stroma, such as T regulatory T-cells (T_{regs}), tumour associated macrophages and myeloid-derived suppressor cells (MDSC) [49]. Similarly, it has been observed that the C5a receptor axis may have a prognostic importance in RCC [49]. In addition, studies have also highlighted that C1 could contribute to RCC progression [49,50]. These findings are in line with our studies that complement system are highly active in *SIGLEC12* RCC formation. This also may position this cancer to respond better to immunotherapy.

Similarly, the suggestion that an enriched JAK-STAT pathway seems to result in *SIGLEC12* associated RC may sound counter-intuitive to the canonical inactivation pathway of its regulation in T-helper cell [36,37]. In this pathway, SHPs acts as a negative

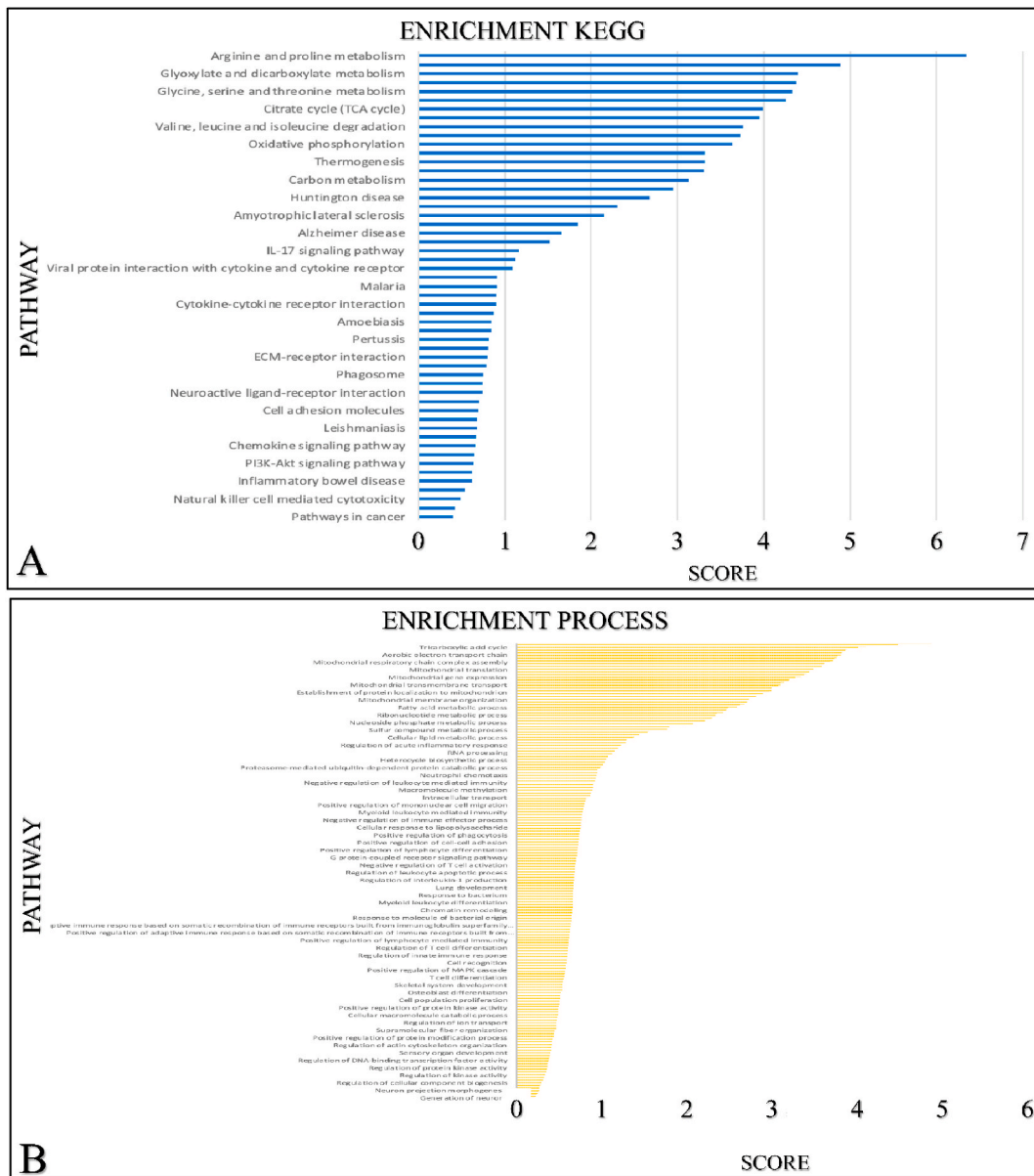


Fig. 8. The *SIGLEC12* enrichment pathway of mRNA expression. Enrichment KEGG (A). Enrichment process (B). Enrichment function (C). Enrichment component (D).

regulator of T-helper cells [37,51,52]. However, in the non-canonical pathway the unphosphorylated STAT in the T-cell heterochromatin are reduced upon STAT's phosphorylation which may be induced by JAK [37,52]. These cascades of events can result in disperse of phosphorylated STAT to bind to a cognitive site of a euchromatin which culminates in gene expression. JAK-STAT pathway has a critical role in CD4⁺ Th cells differentiation into Th1, Th2, Th17 and Tregs [36,37,52]. We could not definitely infer which pathway is involved in our subject matter. This was because the molecular consequences and actions in the signalling of JAK-STAT pathway are complicated with numerous molecular crosstalk [51]. In addition, data available from the enrichment pathways, which are the bases for biological processes and molecular interaction [53,54], Kuo et al. (2021) suggests that a high enrichment score for arginine and proline metabolism [55]. This constitutes a series of non-essential amino acids such as proline, glutamine, asparagine and arginine forming the Pro-Gln-Asn-Arg axis [55,56]. This axis has been implicated in cancer metabolism; for instance, Gln is a potent precursor of nucleotide biosynthesis through the carbamoyl phosphate synthetase-II (CPS-II), aspartate transcarbamylase (ATCase) and Dihydro orotase (CAD) enzyme system. Furthermore, Pro-Gln-Asn-Arg axis has been demonstrated to crosstalk with the tricarboxylic acid (TCA) cycle, thereby metabolizing glucose [56,57]. Approximately 100 years ago, Otto Warburg correctly noted that

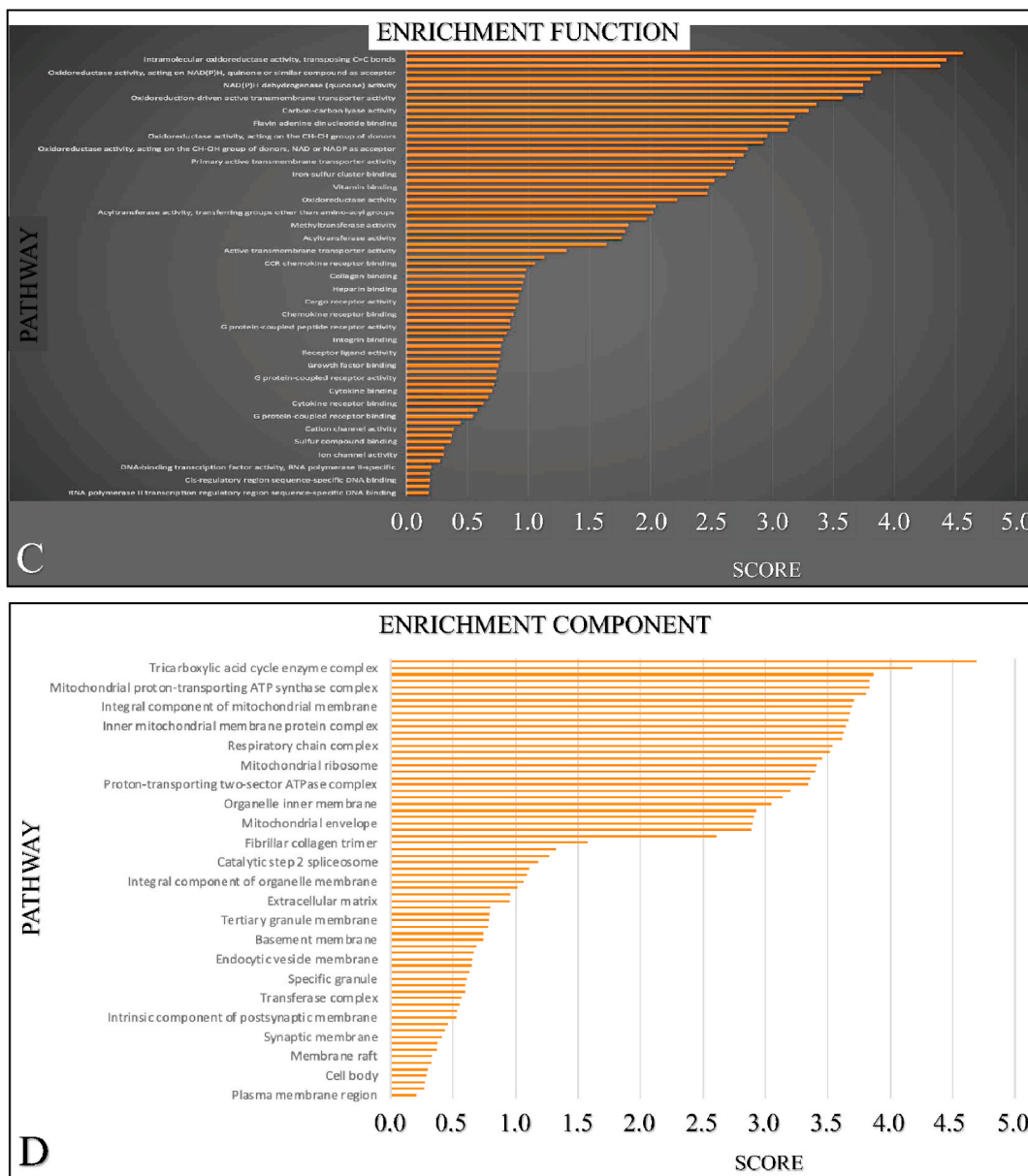


Fig. 8. (continued).

tumour cells increase their demand and usage of glucose [58,59]. This glucose is used to generate ATP and reactive oxygen species (ROS) signalling [60,61]. Similarly, ROS have being described to be a cornerstone in events leading to diseases of protracted duration, such as cancer [62]. Interestingly, with the advent of technology and biochemical studies in animal models, amino acid starvation therapy is now being developed as a useful cancer therapy strategy [55,63]. Tumour heterogeneity and its response to therapy, especially immunotherapy, have become prominent topics of conversation in the last decade [35]. We have established the presence of macrophages in the TME of *SIGLEC12* designated RC. *SIGLEC12* may play a role in tumour progression and the development of cold tumours. Cold tumours, are phenotypically immune deserts cancers characterized by the absence of infiltrate of CD8 + killer T lymphocytes in the tumour parenchymal [64]. In contrast, some cancers are highly immunogenic and [64] exhibit hot tumorigenic tendencies, characterized as a highly immune-inflamed tumour phenotype infiltrated by CD8 + killer T lymphocytes [41]. We hypothesize that the weak correlation observed between immune checkpoint proteins in KIRC patients may render them nonresponsive to targeted immunotherapy, allowing cancer to evade immunosurveillance and leading to poor patient prognosis. Conversely, KIRC patients may be better positioned to respond to immunotherapy, such as CTLA-4 inhibitors (Ipilimumab) and PD-1/PD-L1 (Pembrolizumab) [42,43], due to the relatively positive correlation observed, respectively. It is worth noting, that the peculiarity of the *SIGLEC12* gene, its associated pathways, and functions are totally distinct from other CD33rSiglecs [15]. Thus, the possibility of

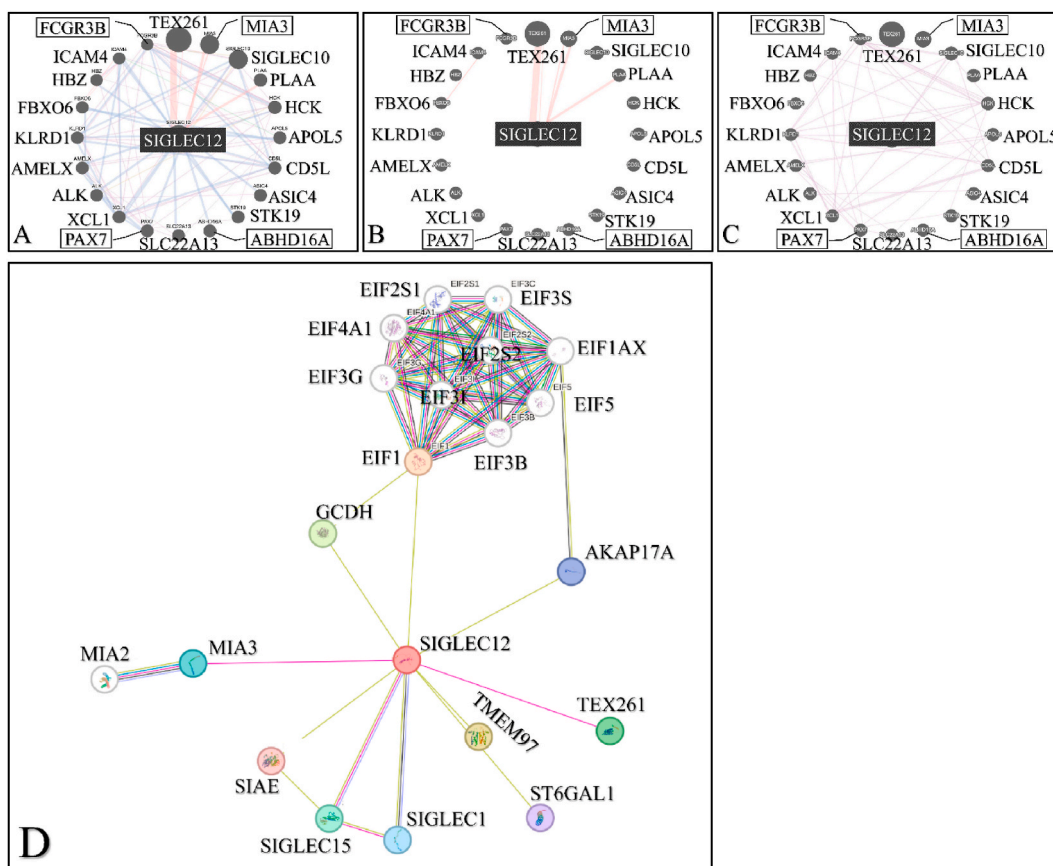


Fig. 9. The potential interconnected communication of *SIGLEC12* with hub genes. Interaction network (A). Physical interaction (B). Co-expression network (C). The connections have different relationships with the genes indicated by different colours. Connection of *SIGLEC12* with hub of genes illustrated in the STRING pathway (D). (For interpretation of the references to colour in this figure legend, the reader is referred to the Web version of this article.)

converting cold tumours into hot tumours may present a novel challenge for immunotherapy [18].

As discussed earlier, multiple signalling cascade, such as autocrine and paracrine pathways, have been highlighted to propagate cancer progression [38,39]. The physical interaction between *SIGLEC12* and phospholipase A2-activating protein (PLAA), a gene that is downregulated in aggressive metastatic ovarian cancer cells [65], suggested an oncogenic function of *SIGLEC12*. Other studies have also implicated PLAA inactivation to the development of lung, and breast cancer [66]. However, we could not establish whether this interaction causes an upregulation or downregulation of PLAA. Similarly, The Human Protein Atlas database have alluded that TEX261 is a prognostic marker in liver and endometrial cancer, with unfavourable outcome [24]. This may imply a significant collaboration between *SIGLEC12* and TEX261 in disease development, given their strong physical interaction. This collaborates our findings on the STRING database tool. Furthermore, the co-expression of Siglec-XII and Siglec10 suggests the interaction of CD33rSiglecs which is interesting. Zhang et al. (2022) noted that altered Siglec10 in 18 normal tissue samples was closely associated with the development and growth of cancer in about 11 tissue samples [67]. Importantly, upregulation of Siglec10 resulted in KIRC (63.4 %) when compared with normal kidney tissues and linked with advanced disease with worse prognosis [67]. Although, the GeneMania data indicated a substantial interaction of factors regulating *SIGLEC12*, however, how they affect downstream molecules in modulating immune system to promote tumorigenesis in RC remain an open question. In addition, EIF, which are the main players in Eukaryotic mRNA translation initiation, are a rate-limiting step in the protein synthesis process [68,69]. Fan et al. (2019) observed in an animal study of RCC malignance that ELF3C depletion resulted in cancer cell proliferation, and shift of tumour cells to G-phase of the cell cycle [70]. Depletion of eIF3C resulted in reduced tumour cell proliferation, increased tumour cell apoptosis, and an increased shift to the G1-phase of the cell cycle when compared with control types [70]. These factors also regulate genes such as AKT, NF κ B and c-Jun, which are pathways that have been implicated in *SIGLEC12* signalling from our study. We propose that the interaction of *SIGLEC12* with these factors results to a primary outcome of rate alteration and dysregulation leading to the proliferation of neoplasms [33]. Furthermore, The Human Protein Atlas database suggests that in RC and testicular cancers expressing Siglec1 gene, the outcome is unfavourable [24]. Similarly, Siglec15 is upregulated in tumours such as COAD, BLCA, KIRP, THCA and KICH [67]. Although Baihui et al. (2020) also acknowledged that the normal sample size compared to tumour sizes was relatively small, we propose that this interaction with *SIGLEC12* is uncommon and contributes to cancer [67].

This first study does have its limitations and raises several important questions. While, previous studies have indicated high expression of *SIGLEC12* in epithelial cells, our investigation only confirmed *SIGLEC12* expression in kidney macrophages. Similarly, we did not delve into the relation between cancer stage and cancer grading or its implications for immunotherapy. The exact mechanism by which *SIGLEC12* functions as an oncogene remains unclear and requires elucidation. Furthermore, we were unable to pinpoint the key driver behind the immunogenicity differences among various RC subtypes. To conduct a more accurate and robust evaluation of this bioinformatics study, we recognize the need for more samples and more detailed clinical analyses.

In conclusion, our study demonstrated the significance of *SIGLEC12* expression in RC prognosis and its potential utility in immunotherapy for disease treatment. Our findings lay the groundwork for further research to identify future targets in the diagnosis and therapeutics of *SIGLEC12*-associated RC. Several aspects of this study warrant further exploration and confirmation.

Declarations

4.1. Ethics approval and consent to participate

Not applicable.

4.2. Consent for publication

Not applicable.

4.3. Availability of data and material

All datasets are publicly available. The Human Protein Atlas database is available in the public domain via the following link: www.proteinatlas.org. HPA datasets used throughout this study are publicly available via the link: <https://www.proteinatlas.org/ENSG00000254521-SIGLEC12>. The online data tool UALCAN is available via <http://ualcan.path.uab.edu>. TCGA dataset is available via the following link: <https://portal.gdc.cancer.gov/>. The TCGA cancers datasets selected for study can be found via the following link: <https://www.cancer.gov/about-nci/organization/ccg/research/structural-genomics/tcga/studied-cancers>. The Kaplan–Meier plotter (KM plotter), is publicly available via <https://kmplot.com/analysis>. Tumor Immune Estimation Resource (TIMER) is an online tool available in the public domain via <https://cistrome.shinyapps.io/timer/>. cBioPortal is available via the link http://cbioportal.org/cancer_study_list=kirc_tcga_pan_can_atlas_2018&tab_index=tab_visualize&case_set_id=kirc_tcga_pan_can_atlas_2018_all&Action=Submit&gene_list=SIGLEC12. Gene set enrichment analysis (GSEA) software is available to the public via the following link: <https://www.gsea-msigdb.org/>. GeneMania is available in the public domain via <https://genemania.org>. Data regarding specifically Siglec12 outcomes can be found at <https://genemania.org/search/homo-sapiens/siglec12>.

Funding

There is no funding associated with this work.

Data availability statement

No data was used for the research described in the article.

CRedit authorship contribution statement

Amobichukwu K. Ogbodo: Data curation, Methodology, Writing – original draft, Writing – review & editing. **Denis Mustafov:** Data curation, Methodology, Writing – review & editing. **Mohit Arora:** Methodology, Supervision, Writing – review & editing. **George I. Lambrou:** Data curation, Methodology, Writing – review & editing. **Maria Braoudaki:** Methodology, Supervision, Writing – review & editing, Conceptualization. **Shoib S. Siddiqui:** Conceptualization, Data curation, Methodology, Supervision, Writing – review & editing.

Declaration of competing interest

The authors declare that they have no known competing financial interests or personal relationships that could have appeared to influence the work reported in this paper.

Acknowledgements

None.

References

- [1] J. Huang, et al., A Global trend analysis of kidney cancer incidence and mortality and their associations with smoking, alcohol consumption, and metabolic syndrome, *Eur Urol Focus* 8 (1) (2022) 200–209.
- [2] F. Bray, et al., Global cancer statistics 2018: GLOBOCAN estimates of incidence and mortality worldwide for 36 cancers in 185 countries, *CA Cancer J Clin* 68 (6) (2018) 394–424.
- [3] H. Sung, et al., Global cancer statistics 2020: GLOBOCAN estimates of incidence and mortality worldwide for 36 cancers in 185 countries, *CA Cancer J Clin* 71 (3) (2021) 209–249.
- [4] P. Li, et al., Regional geographic variations in kidney cancer incidence rates in European countries, *Eur. Urol.* 67 (6) (2015) 1134–1141.
- [5] G. Scelo, T.L. Larose, Epidemiology and risk factors for kidney cancer, *J. Clin. Oncol.* 36 (36) (2018). JCO2018791905.
- [6] W.M. Linehan, et al., Molecular diagnosis and therapy of kidney cancer, *Annu. Rev. Med.* 61 (2010) 329–343.
- [7] T.D. Treger, et al., The genetic changes of Wilms tumour, *Nat. Rev. Nephrol.* 15 (4) (2019) 240–251.
- [8] D.A. Siegel, et al., Cancer incidence rates and trends among children and adolescents in the United States, 2001–2009, *Pediatrics* 134 (4) (2014) e945–e955.
- [9] H. Laubli, et al., Tools to study and target the Siglec-sialic acid axis in cancer, *FEBS J.* 288 (21) (2021) 6206–6225.
- [10] I. Ibarlucea-Benitez, et al., Siglecs-7/9 function as inhibitory immune checkpoints in vivo and can be targeted to enhance therapeutic antitumor immunity, *Proc Natl Acad Sci U S A* 118 (26) (2021).
- [11] S.S. Siddiqui, Non-canonical roles of Siglecs: beyond sialic acid-binding and immune cell modulation, *Mol Aspects Med* 90 (2023) 101145.
- [12] V. Padler-Karavani, et al., Rapid evolution of binding specificities and expression patterns of inhibitory CD33-related Siglecs in primates, *FASEB J* 28 (3) (2014) 1280–1293.
- [13] B.S. Bochner, N. Zimmermann, Role of siglecs and related glycan-binding proteins in immune responses and immunoregulation, *J. Allergy Clin. Immunol.* 135 (3) (2015) 598–608.
- [14] O.J. Adams, et al., Targeting sialic acid-Siglec interactions to reverse immune suppression in cancer, *Glycobiology* 28 (9) (2018) 640–647.
- [15] S.S. Siddiqui, et al., Human-specific polymorphic pseudogenization of SIGLEC12 protects against advanced cancer progression, *FASEB Bioadv* 3 (2) (2021) 69–82.
- [16] R. Flores, et al., Siglec genes confer resistance to systemic lupus erythematosus in humans and mice, *Cell. Mol. Immunol.* 16 (2) (2019) 154–164.
- [17] N. Mitra, et al., SIGLEC12, a human-specific segregating (pseudo)gene, encodes a signaling molecule expressed in prostate carcinomas, *J. Biol. Chem.* 286 (26) (2011) 23003–23011.
- [18] Z. Yu, et al., Identification and characterization of S2V, a novel putative siglec that contains two V set Ig-like domains and recruits protein-tyrosine phosphatases SHPs, *J. Biol. Chem.* 276 (26) (2001) 23816–23824.
- [19] B. Yngvadottir, et al., A genome-wide survey of the prevalence and evolutionary forces acting on human nonsense SNPs, *Am. J. Hum. Genet.* 84 (2) (2009) 224–234.
- [20] M.V. Olson, When less is more: gene loss as an engine of evolutionary change, *Am. J. Hum. Genet.* 64 (1) (1999) 18–23.
- [21] J.M. Akey, et al., Interrogating a high-density SNP map for signatures of natural selection, *Genome Res.* 12 (12) (2002) 1805–1814.
- [22] L.B. Barreiro, et al., Natural selection has driven population differentiation in modern humans, *Nat. Genet.* 40 (3) (2008) 340–345.
- [23] P.R. Crocker, P. Redelinghuys, Siglecs as positive and negative regulators of the immune system, *Biochem. Soc. Trans.* 36 (Pt 6) (2008) 1467–1471.
- [24] P.J. Thul, et al., A subcellular map of the human proteome, *Science* 356 (6340) (2017).
- [25] D.S. Chandrashekar, et al., UALCAN: a portal for facilitating tumor subgroup gene expression and survival analyses, *Neoplasia* 19 (8) (2017) 649–658.
- [26] Z. Shafat, et al., Identification of the key miRNAs and genes associated with the regulation of non-small cell lung cancer: a network-based approach, *Genes* 13 (7) (2022).
- [27] B.P. Lewis, et al., Prediction of mammalian microRNA targets, *Cell* 115 (7) (2003) 787–798.
- [28] H. Dweep, et al., miRWalk–database: prediction of possible miRNA binding sites by "walking" the genes of three genomes, *J. Biomed. Inf.* 44 (5) (2011) 839–847.
- [29] T.P. Lu, et al., miRSystem: an integrated system for characterizing enriched functions and pathways of microRNA targets, *PLoS One* 7 (8) (2012) e42390.
- [30] C.H. Gao, G. Yu, P. Cai, ggVennDiagram: an intuitive, easy-to-use, and highly customizable R package to generate Venn diagram, *Front. Genet.* 12 (2021) 706907.
- [31] A. Nagy, et al., Validation of miRNA prognostic power in hepatocellular carcinoma using expression data of independent datasets, *Sci. Rep.* 8 (1) (2018) 9227.
- [32] M. Kanehisa, S. Goto, KEGG: kyoto encyclopedia of genes and genomes, *Nucleic Acids Res.* 28 (1) (2000) 27–30.
- [33] H. Zhang, et al., Integrative analysis of the expression of SIGLEC family members in lung adenocarcinoma via data mining, *Front. Oncol.* 11 (2021) 608113.
- [34] J. Montojo, et al., GeneMANIA Cytoscape plugin: fast gene function predictions on the desktop, *Bioinformatics* 26 (22) (2010) 2927–2928.
- [35] T. Long, et al., Identification of differentially expressed genes and enriched pathways in lung cancer using bioinformatics analysis, *Mol. Med. Rep.* 19 (3) (2019) 2029–2040.
- [36] A. Franceschini, et al., STRING v9.1: protein-protein interaction networks, with increased coverage and integration, *Nucleic Acids Res.* 41 (2013) D808–D815 (Database issue).
- [37] O.V. Kovaleva, et al., Tumor associated macrophages in kidney cancer, *Anal. Cell Pathol.* 2016 (2016) 9307549.
- [38] J. Gao, et al., Integrative analysis of complex cancer genomics and clinical profiles using the cBioPortal, *Sci. Signal.* 6 (269) (2013) p11.
- [39] E. Cerami, et al., The cBio cancer genomics portal: an open platform for exploring multidimensional cancer genomics data, *Cancer Discov.* 2 (5) (2012) 401–404.
- [40] A. Subramanian, et al., Gene set enrichment analysis: a knowledge-based approach for interpreting genome-wide expression profiles, *Proc Natl Acad Sci U S A* 102 (43) (2005) 15545–15550.
- [41] L. Esserman, Y. Shieh, I. Thompson, Rethinking screening for breast cancer and prostate cancer, *JAMA* 302 (15) (2009) 1685–1692.
- [42] S. Oliveto, et al., Role of microRNAs in translation regulation and cancer, *World J. Biol. Chem.* 8 (1) (2017) 45–56.
- [43] S. Liu, et al., microRNA-133b represses the progression of lung cancer through inhibiting SOX9/ β -catenin signaling pathway, *Int. J. Clin. Exp. Pathol.* 13 (9) (2020) 2270–2279.
- [44] L. Wang, et al., IFN- γ and TNF- α synergistically induce mesenchymal stem cell impairment and tumorigenesis via NF κ B signaling, *Stem Cell.* 31 (7) (2013) 1383–1395.
- [45] M. Mojic, K. Takeda, Y. Hayakawa, The dark side of IFN- γ : its role in promoting cancer immunoevasion, *Int. J. Mol. Sci.* 19 (1) (2017).
- [46] D.J. Gough, et al., IFN γ signaling-does it mean JAK-STAT? Cytokine Growth Factor Rev. 19 (5–6) (2008) 383–394.
- [47] E. Niccolai, et al., Intra-tumoral IFN- γ -producing Th22 cells correlate with TNM staging and the worst outcomes in pancreatic cancer, *Clin. Sci. (Lond.)* 130 (4) (2016) 247–258.
- [48] M.M. Markiewski, J.D. Lambris, Is complement good or bad for cancer patients? A new perspective on an old dilemma, *Trends Immunol.* 30 (6) (2009) 286–292.
- [49] B. Reese, et al., Complement as prognostic biomarker and potential therapeutic target in renal cell carcinoma, *J. Immunol.* 205 (11) (2020) 3218–3229.
- [50] Z. Fishelson, et al., Obstacles to cancer immunotherapy: expression of membrane complement regulatory proteins (mCRPs) in tumors, *Mol. Immunol.* 40 (2–4) (2003) 109–123.
- [51] L.A. Pozzi, J.W. Maciaszek, K.L. Rock, Both dendritic cells and macrophages can stimulate naive CD8 T cells in vivo to proliferate, develop effector function, and differentiate into memory cells, *J. Immunol.* 175 (4) (2005) 2071–2081.
- [52] A.M. Morch, et al., Coreceptors and TCR signaling - the strong and the weak of it, *Front. Cell Dev. Biol.* 8 (2020) 597627.
- [53] L. Hodgkinson, R.M. Karp, Optimization criteria and biological process enrichment in homologous multiprotein modules, *Proc Natl Acad Sci U S A* 110 (26) (2013) 10872–10877.
- [54] I. Rodchenkov, et al., Pathway Commons 2019 Update: integration, analysis and exploration of pathway data, *Nucleic Acids Res.* 48 (D1) (2020) D489–d497.
- [55] M.T. Kuo, et al., Targeting the proline-glutamine-asparagine-arginine metabolic Axis in amino acid starvation cancer therapy, *Pharmaceuticals* 14 (1) (2021).

- [56] W. Liu, J.M. Phang, Proline dehydrogenase (oxidase) in cancer, *Biofactors* 38 (6) (2012) 398–406.
- [57] J. Nomme, Y. Su, A. Lavie, Elucidation of the specific function of the conserved threonine triad responsible for human L-asparaginase autocleavage and substrate hydrolysis, *J. Mol. Biol.* 426 (13) (2014) 2471–2485.
- [58] O. Warburg, F. Wind, E. Negelein, The metabolism of tumors in the body, *J. Gen. Physiol.* 8 (6) (1927) 519–530.
- [59] O. Warburg, The metabolism of carcinoma Cells1, *J. Cancer Res.* 9 (1) (1925) 148–163.
- [60] J. Eniafe, S. Jiang, The functional roles of TCA cycle metabolites in cancer, *Oncogene* 40 (19) (2021) 3351–3363.
- [61] W.S. da-Silva, et al., Mitochondrial bound hexokinase activity as a preventive antioxidant defense: steady-state ADP formation as a regulatory mechanism of membrane potential and reactive oxygen species generation in mitochondria, *J. Biol. Chem.* 279 (38) (2004) 39846–39855.
- [62] C.R. Reczek, N.S. Chandel, The two faces of reactive oxygen species in cancer, *Annu. Rev. Cell Biol.* 1 (1) (2017) 79–98.
- [63] M. Butler, L.T. van der Meer, F.N. van Leeuwen, Amino acid depletion therapies: starving cancer cells to death, *Trends Endocrinol Metab* 32 (6) (2021) 367–381.
- [64] D.S. Chen, I. Mellman, Elements of cancer immunity and the cancer-immune set point, *Nature* 541 (7637) (2017) 321–330.
- [65] G.L. Johnson, R. Lapadat, Mitogen-activated protein kinase pathways mediated by ERK, JNK, and p38 protein kinases, *Science* 298 (5600) (2002) 1911–1912.
- [66] S. Sasaki, et al., Molecular processes of chromosome 9p21 deletions in human cancers, *Oncogene* 22 (24) (2003) 3792–3798.
- [67] B. Li, et al., Expression signature, prognosis value, and immune characteristics of Siglec-15 identified by pan-cancer analysis, *OncolImmunology* 9 (1) (2020) 1807291.
- [68] A.G. Hinnebusch, The scanning mechanism of eukaryotic translation initiation, *Annu. Rev. Biochem.* 83 (2014) 779–812.
- [69] P. Hao, et al., Eukaryotic translation initiation factors as promising targets in cancer therapy, *Cell Commun. Signal.* 18 (1) (2020) 175.
- [70] M. Fan, et al., Upregulated expression of eIF3C is associated with malignant behavior in renal cell carcinoma, *Int. J. Oncol.* 55 (6) (2019) 1385–1395.